

## DC Conduction Processes in Electron Beam Evaporated Bromoaluminium Phthalocyanine Thin Films

M. E. Azim Araghi, S. Riyazi\*, S. Pourteimoor;  
Physics Department, Kharazmi University

### Abstract

In the present study, we investigated DC conduction mechanism of electron beam evaporated Bromoaluminium phthalocyanine (BrAlPc) thin films using aluminum and gold electrodes. The current-voltage characteristics of sandwich type device are evaluated for the temperature range 298-413K under dark conditions. It is observed that the current passing through the device is increased by increasing temperature at the same voltage in the range of 0-6v. It is found that at lower voltages about 0 to 2v, the current-voltage characteristics demonstrate Ohmic behavior, while the space charge limited current (SCLC) becomes apparent at higher voltages about 2 to 6v, which is restricted by single discrete trapping level. We obtained more than one linear region in the temperature dependence of electrical conductivity. Also, the values of charge carrier mobility and the activation energy of device are evaluated.

### Introduction

Thin films of organic materials having semiconductor properties are being extensively studied due to the very promising applications of organic electronics such as organic light-emitting diodes (OLEDs) [1], gas sensors [2], organic thin film transistors (OTFTs) [3] and solar cells [4]. These applications depend extremely on the conductivity of organic molecular material, and charge transport processes [5]. Charge transport mechanism in organic semiconductor materials is mainly determined by hopping process between two localized molecular states as seen in amorphous semiconductors [6].

---

**Keywords:** Bromoaluminium phthalocyanine; Thin films; Organic semiconductor; Conduction mechanism

Received: 23 April 2013

Revised 15 Dec 2013

\*Corresponding author: sobhnaz@gmail.com

More recent experimental work has supported a hopping model, while theoretical studies may be found arguing for either hopping model or a band model [7], [8]. Gould [9] reports that band theory is appropriate for mobilities greater than  $10^{-4} \text{ m}^2 \text{ V}^{-1} \text{ s}^{-1}$  while for lower mobility hopping dominates.

Among organic semiconductors, the metal-phthalocyanines (MPc's) are one of the best candidates for novel molecular electronic devices [10]. They have a great technological potential in areas related to intrinsic semiconductors and conductive polymers [11]. Much of the research into the semiconductor behavior of metal-phthalocyanines (MPc's) has been carried out using interdigital planar or sandwich devices [12]. Semiconductor behavior of these thin films is p-type. However, addition of electron withdrawing functional groups, particularly fluorine, can alter molecular orbital structure drastically, leading to n-type phthalocyanine [13].

MPc's films have little intrinsic conductivity and their observed conductivity depends strongly on atmospheric chemical species, particularly oxidizing or reducing gases [9]. There are several conduction mechanisms that have been reported for MPc thin films that significantly depend on the type of metallic contact and also depend on the applied voltage across the specimen as well as temperature of interest [14]. The electrical properties of the metal phthalocyanine deposited between gold and lead electrodes have been investigated by Varghese et al [15] and it has been found that the current-voltage characteristics show Ohmic conduction at lower voltages followed by space charge limited current at higher voltages.

However, few studies have been conducted on the halogenated Pc's, which have remarkable morphological and thermal stability over a large range of temperature compared to unhalogenated Pc's [16]. Though, Bromoaluminium phthalocyanine (BrAlPc) is a halogenated phthalocyanine very few work has been performed on electrical properties of this material. Here, we attempt to explain the DC conduction mechanism of electron beam evaporated thin films of BrAlPc using aluminum and gold electrodes. Since phthalocyanines are photoconductive [17] measurements were carried out in dark room in the temperature range 298-413 K.

## Experimental details

### 1. Synthesis

Bromoaluminium phthalocyanine material was prepared in our laboratory in the following way. A mixture of 40 g phthalonitrile, 10 g  $\text{AlBr}_3$  and 200 ml quinoline (doubly distilled and deoxygenated under a nitrogen atmosphere) were refluxed for 1.5 h. The resulting hot mixture was then filtered in a glass filter. It was then cooled to  $0^\circ\text{C}$  and filtered. The solid thus isolated was then washed sequentially with toluene, carbon tetrachloride and acetone, and then dried under vacuum at  $110^\circ\text{C}$ . The chemically prepared BrAlPc contains significant amounts of impurities, therefore purification is essential. The entrainer sublimation technique has been carried out for purification.

### 2. Thin films preparation and characterization

A microscopic glass slides with dimensions of  $1.5 \times 1 \times 0.2 \text{ cm}^3$  were used as substrates. Prior to deposition of BrAlPc thin films, the glass substrates were cleaned using acetone and deionized water and then dried in order to avoid contamination. Thin films were coated on pre-cleaned glass substrates using electron beam gun evaporation technique (HIND HIVAC, EBG-PC-3K). Deposition was performed at a base pressure of  $10^{-5}$  mbar onto substrates maintained at room temperature using a molybdenum boat. Thickness of each layer was monitored by a quartz crystal system (HIND HIVAC, DTM\_101). The aluminum and gold electrodes were evaporated at a deposition rate of 0.7 nm/s with a thickness of 80 nm, while deposition rate of BrAlPc thin films were 1 nm/s with a thickness of 100 nm. The active area of device is about  $5 \times 10^{-5} \text{ m}^2$ . The electrical contacts were equipped with copper wires to the metal electrodes using silver paint. A schematic diagram of fabricated device and molecular structure of BrAlPc is shown in Figure. 1.

The DC electrical measurements of the fabricated device were performed using a Keithly 610C electrometer in the temperature range 298-413 K. To avoid photoelectric effects, all the measurements were carried out in a dark room.

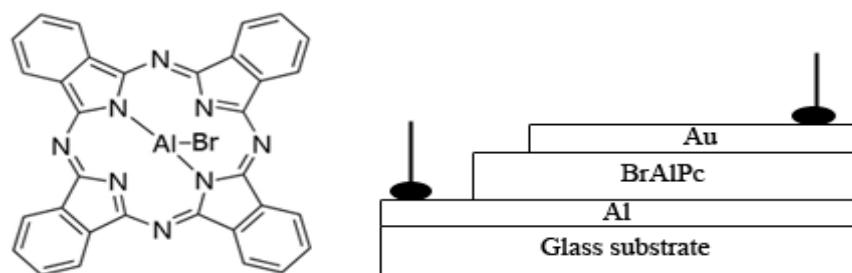


**Figure1.** Molecular structure of BrAlPc and schematic diagram of Al-BrAlPc-Au device

## Results and discussion

### 1. Conduction mechanism

The dark current-voltage characteristics ( $I$ - $V$ ) of the BrAlPc thin film with thickness 100 nm sandwiched between aluminum and gold electrodes at different temperatures is shown in Figure. 2. The device is allowed to equilibrate at each temperature and voltage. Figure 2 shows that the dark current increases as the temperature increases and device has a good performance at higher temperatures.

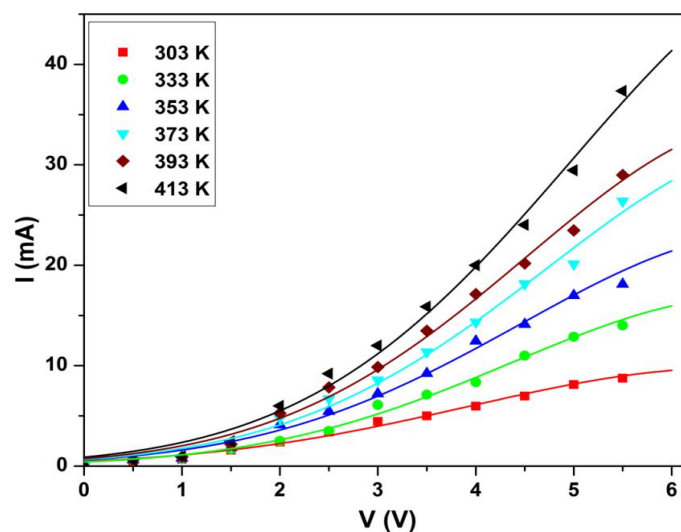


**Figure2.** Dark current-voltage characteristics of Al-BrAlPc-Au device at different temperatures

Device shows a good performance at higher temperatures.

Figure. 3 shows the current-voltage characteristics of Al-BrAlPc-Au device at 393 and 413 K in logarithmic scale.

At low applied voltages, conduction obeys Ohm's law, while at higher voltages space charge limited conduction (SCLC) was the dominated mechanism.

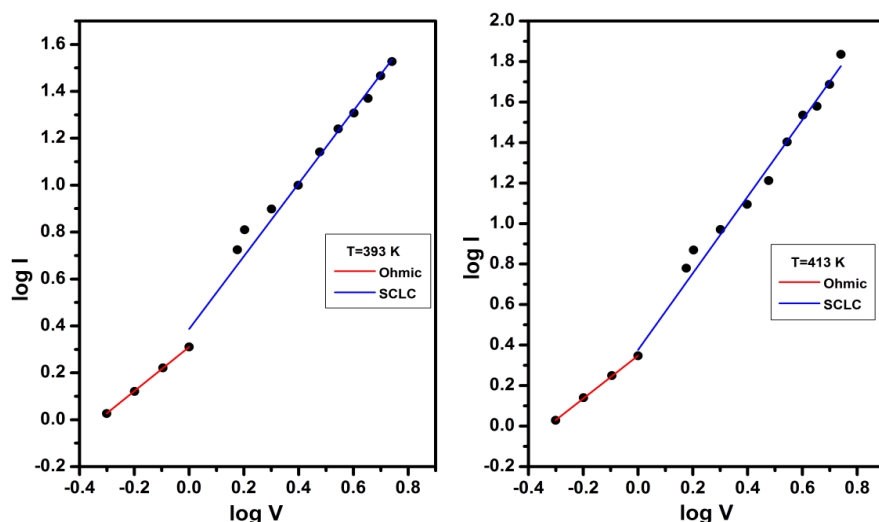


**Figure3. Current-Voltage characteristics of Al-BrAlPc-Au device at 393 and 413 K in logarithmic presentation**

There are two distinct regions of conduction for each characteristic curve. These regions are typical of Ohmic conduction below transition voltage ( $V_t$ ) and the space-charge limited conduction (SCLC) at voltage above transition voltage, as qualitatively shown in Figure. 4. The slope of about unity for the curves at low fields indicates Ohmic conduction. Above a critical field the current increased monotonically, indicating several conduction mechanisms. Included among such conduction phenomena are Schottky-type barrier-controlled conduction, Poole-Frenkel conduction and bulk-limited space charge conduction. Since the I-V characteristics indicate a bulk conduction process, a Schottky-type barrier-controlled mechanism may not be possible with the present results. For Poole-Frenkel conduction, there must be a linear relation between  $J/T^2$  versus  $1000/T$ ,  $J$  is the current density and  $T$  is the temperature, however such dependence is not observed in present case.

At the low electric field, charge transport by thermal carrier dominates and no net chargers built up in the film. Therefore, at low voltages, thermally generated holes are few and the injected hole density is small so that the overall behavior becomes Ohmic. As the voltage is increased, the number of injected holes increases, which overcomes the transport capabilities of BrAlPc, hence giving rise to the accumulation of a positive space charge near the anode. The field due this space charge is responsible for limiting

the current and giving rise to SCLC conduction. SCLC is a bulk limited process and depends only on the transport of the carriers and on the trapping centers in the deposited films. These conduction regimes have a direct impact on the sensing properties Of MPC's; the Ohmic contact resistance that may occur between the electrode and the film may be removed by operating the sensor in the SCLC regime, leading to more consistent and stable sensor behavior [18].

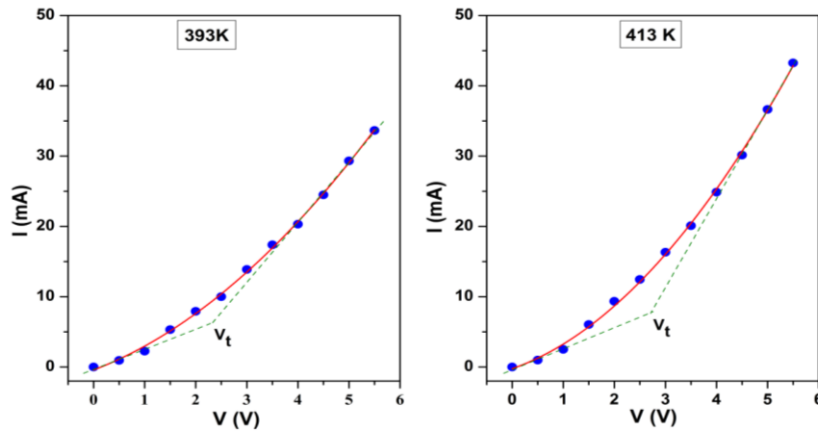


**Figure4. Current-Voltage characteristics of Al-BrAlPc-Au device at 393 and 413 K**  
The threshold voltage ( $V_t$ ) indicates the turn from Ohmic to space charge limited current (SCLC)

In the Ohmic region, current density  $J$  may be expressed as [19]

$$J = en\mu \frac{V}{d} \quad (1)$$

where  $e$  is the electronic charge,  $n$  is the free carrier density,  $\mu$  is the charge carrier mobility,  $V$  is the applied voltage and  $d$  is the film thickness. In the SCLC region, current density  $J$  can be described by the Mutt-Gurney square law [20] according to:

$$J = \frac{9}{8} \epsilon_0 \epsilon_r \mu \frac{V^2}{d^3} \quad (2)$$

where  $\epsilon_0$  and  $\epsilon_r$  represents the permittivity for free space and organic semiconductor respectively,  $\mu$  charge carrier mobility,  $d$  film thickness and  $V$  is the applied voltage. In general, variation of current with voltage in SCLC region can be described as:

$$I \propto V^n \quad (3)$$

Where the index  $n$  has values  $\geq 2$  [14], which may be determined from the following expression

$$n = \frac{\ln(I_2) - \ln(I_1)}{\ln(V_2) - \ln(V_1)} \quad (4)$$

where  $I_1$  and  $I_2$  are currents evaluated at voltages  $V_1$  and  $V_2$ , respectively. The numerical

value of the index  $n$  was found to be associated with the nature of traps [21] and the sample temperature [22]. Moreover, the amount of oxygen content within phthalocyanine film was found to have great influence on the value of the index  $n$  [23]. In particular, high transport processes (index  $n > 2$ ) are related to traps and their distribution within the band gap. We have found that the value of  $n$  is approximately 2 (quadratic dependence of the current on voltage) in the SCLC region that indicates trap-free space charge-limited current (TFSCLC) conduction [24]. Note that the slope equal to 2 does not imply the absence of traps in the materials but rather that they are all filled. These traps are localized energy states which exist within the band gap that may be generated by structural defects [25], impurities [26], self-trapping [27], Geminate pairs [28] and  $O_2$  molecules [14].

Figure. 5 shows the variation of natural logarithmic of current versus inverse of temperature at constant applied voltages which yields a linear plot. The slope of the lines enables to distinguish between a single discrete trapping level and traps at exponentially distributed level which exist in energy space below the low unoccupied molecular orbital (LUMO), conduction band edges, and above high occupied molecular orbital (HOMO), valance band edges.

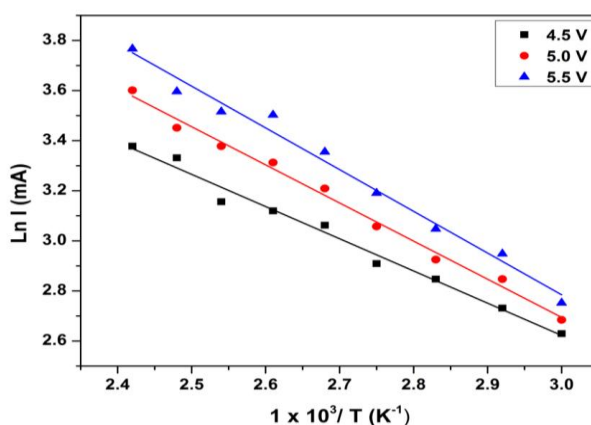


**Figure 5. Natural logarithmic current versus inverse of temperature characteristics of BrAlPc films at 4.5, 5.0 and 5.5 volts. Almost the same slopes indicate the existence of discrete trapping level**

A constant slope will be obtained for a single trapping level, which yields its depth below the conduction band. Also, there will be clear variation in the slopes for an exponentially trap distribution [29]. From figure 5, different curves with almost same

slopes were obtained, which indicates that BrAlPc based thin film device has a single discrete trapping level. Most frequently, many researchers assume an exponential distribution of traps in the energy band [30-32]. However, such distribution may not be possible with the present results.

Traps affect the charge transport properties since the trapped charge carriers do no longer take part in drift and diffusion currents. However, their columbic charge will influence the electric field distribution in a device and therewith the transport. Thus, traps impose restrictions on space charge limited current. Under the influence of traps, equation (2) can be modified as

$$J = \frac{9}{8} \epsilon_0 \epsilon_r \theta \mu \frac{V^2}{d^3} \quad (5)$$

where  $\theta$  is the trap factor which is defined as the ratio of free hole,  $p_0$ , carriers density, to the total carrier density of free and trapped hole,  $p_t$ . Therefore, the equation for trap factor is written as

$$\theta = \frac{p_0}{p_0 + p_t} \quad (6)$$

Experimentally, the value of trap factor can be calculated as

$$\theta = \frac{J_1}{J_2} \quad (7)$$

where  $J_1$  and  $J_2$  are the ratio of current densities at the beginning and at the end of the square law region [33]. Figure. 6 shows the variation of trap factor with temperature. It is seen that the values of  $\theta$  nearly remain unchanged at low temperature and then there is a steep increase in its value with increasing temperature. This behavior may be justified by the fact that at higher temperature trapped charge carriers acquire additional energy enabling them to overcome the barrier height of shallow traps. As a result, more trapped charge carriers are released from their localized states.

## 2. Carrier mobility

The behavior of free carriers under the influence of voltage for devices having shallow traps can be assessed by evaluating the mobility of these carriers. To determine it, a large number of methods have been developed such as time of flight (TOF) [34] method, surface acousto-electric traveling wave (SAW) method [35] and SCLC method.



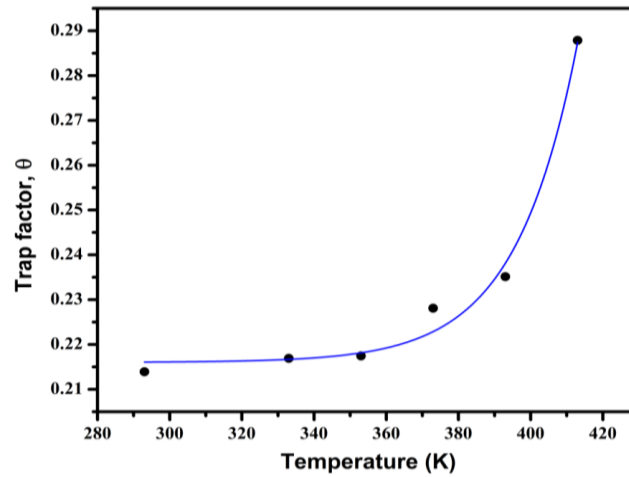


**Figure 6. Variation of trap factor ( $\theta$ ) with temperature for Al-BrAlPc-Au device. At low temperature, trap factor is relatively unchanged but when temperature increases trap factor changes nonlinearly**

Experimental work to date in disordered organic semiconductors in the literature [36–38] mainly applies the general SCLC theory without or with traps in order to extract the charge carrier mobility. It is, therefore, preferred to characterize organic semiconductor devices by using SCLC measurements, which are close to the device operational conditions [39]. Using Eq. 5 and assuming that  $\epsilon_r = 3.6$  for most phthalocyanines [40], charge transport mobility of BrAlPc films was determined as  $2.7 \times 10^{-7} \text{ cm}^2/(\text{V}\cdot\text{s}) < \mu < 1.17 \times 10^{-6} \text{ cm}^2/(\text{V}\cdot\text{s})$ . The low mobility indicates that charge transport in BrAlPc thin films can be described as subsequent inter-chain hopping from localized to localized states. This localization and large density of trap states, potential for collisions, scattering, and delays contributes to the low mobilities of organic charge transport materials.

### 3. Activation energy

The activation energy of the device is calculated using the temperature dependence of the conductivity that can be expressed as:

$$\sigma_{\text{DC}} = \sigma_0 \exp\left(-\frac{E}{K_B T}\right) \quad (8)$$

$$\text{Ln}(\sigma_{\text{DC}}) = \text{Ln}(\sigma_0) - \left(\frac{E}{K_B T}\right) \quad (9)$$

where  $\sigma$  is the DC electrical conductivity at temperature  $T$ ,  $E$  is the activation energy and  $K_B$  is the Boltzmann constant. Figure. 7 shows the temperature dependence of the conductivity in Ohmic region for BrAlPc thin films.

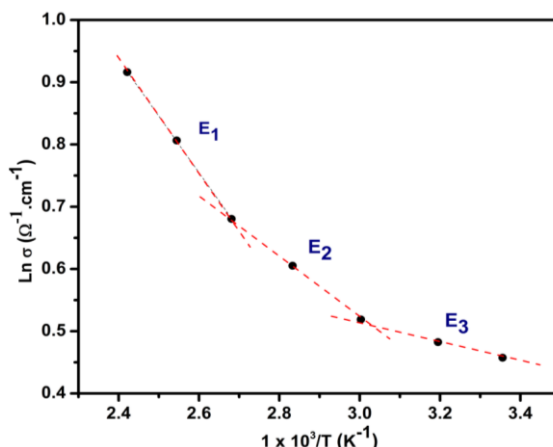


**Figure 7.** Plot of  $\ln(\sigma)$  versus  $1000/T$  for Al-BrAlPc-Au device.  $E_1$ ,  $E_2$  and  $E_3$  are activation energies in the intrinsic region and impurity scattering regions, respectively

The slopes of lines in figure 7 give the activation energy of the BrAlPc thin films. From this figure, it is clear that there are three linear regions that corresponding to three activation energies  $E_1$ ,  $E_2$  and  $E_3$ . The activation energy  $E_1 = 0.96$  eV corresponds to an intrinsic generation process, i.e. the resonant energy involved in a short lived excited state.  $E_2 = 0.57$  eV and  $E_3 = 0.18$  eV is associated with impurity conduction, i.e. a short lived charge transfer between the impurity and the complex [41]. This behavior was also reported in thin films of indium phthalocyanine chloride, InPcCl, [42] nickel phthalocyanine, NiPc, [43] and magnesium phthalocyanine, MgPc [44].

## Conclusion

In summary, the DC conduction mechanism of electron beam evaporated BrAlPc thin films has been investigated. The current-voltage characteristics are determined as a function of temperature, which are then explained by employing trapped space charge limited current model. Trap factor, charge carriers mobility and activation energy of BrAlPc thin film were evaluated. It has been observed that device is nonlinear in its electrical response and the current increased by increasing temperature. The current transport mechanisms of device were found to be Ohmic at low applied voltages and followed by a space charge limited current (SCLC) at higher voltages. Temperature dependence of natural logarithm of current confirmed the existence of trap states within the band gap. The characteristic parameter trap factor,  $\theta$ , was found to be nearly unchanged at low temperatures and there is a steep increase in its value with increasing

temperature. Also, in the temperature dependence of electrical conductivity plot, more than one linear region was obtained, which confirms the existence of trap states.

## References

1. S. R. Forrest, *Chem. Rev.* 97 (2001) 681.
2. M. Jafari, M. E. Azim-Araghi, S. Barhemat, *J. Mater. Sci.* 47(2012) 1992.
3. Y. Wang, K. Lee, J. Oh, S. Kim, M. Lee, H. Kim, (2012) Doi: 10.1007/s13233-013-1102-x.
4. K. Vasseur, Barry P. Rand, D. Cheyns, K. Temst, L. Froyen, Paul Heremans, J., *Phys. Chem. Lett.* 3 (2012) 2395.
5. D. A. Evans, H. J. Steiner, S. Evans, R. Middleton, T. S. Jones, S. Park, T. U Kampen, D. R. T. Zahn, G. abailh and I. T. McGovern, *J. Phys.: Condens. Matter* 15 (2003) 2729.
6. R. Schmechel, H. V. Seggern, *Phys. Stat. Sol. A.* 201 (2004) 1215.
7. R. Coehoorn, W. F. Pasveer, P. A. Bobbert, M. A. Michels, *J. Phys. Rev. B* 72 (2005) 155206.
8. J. E. Norton, J. L. Bredas, *J. Chem. Phys.* 128 (2008) 034701.
9. R. D. Gould, *Coord. Chem. Rev.* 156 (1996) 237.
10. Mutabar Shah, Kh. S. Karimov, M. H. Sayyad, *Semicond. Sci. Technol.* 25(2010) 075014.
11. J. Garcia, A. Gonzalez, A. Gouloumis, E. M. Maya, M. D. Perez, B. D. Rey, P. Vazquez, T. Torres, *Tr. J. of Chemistry* 22 (1998) 23.
12. M. E. Azim-Araghi, A. Krier, *Pure Appl. Opt.* 6 (1997) 443.
13. S. P. Keizer, J. Mack, B. A. Bench, S. M. Gorun, M. J. Stillman, *J. Am. Chem. Soc.* 125 (2003) 7067.
14. A. M. Saleha, A. K. Hassan, R. D. Gould, *Journal of Physics and Chemistry of Solids* 64 (2003) 1297.
15. Abraham C. Varghese, C. S. Menon, *J. Mater. Sci. Mater. Electron.* 17 (2006) 149.
16. A. Napier, R. A. Collins, *Phys. Stat. Sol. A* 144 (1994) 91.
17. L. F. Santos, R. M. Faria, T. Del Cano, J. A. de Saja, C. J. L. Constantino, C. A. Amorim and S Mergulhao, *J. Phys. D: Appl. Phys.* 41 (2008) 125107.
18. A. Wilson, R. A. Collins, *Sens. Actuators* 12 (1987) 389.
19. Abraham C. Varghese, C. S. Menon, *J. Mater. Sci. Mater. Electron.* 18 (2007) 587.
20. M. Abkowitz, J. S. Facci, J. Rehm, *J. Appl. Phys.* 83 (1998) 2670.

21. J. G. Simmons, *J. Phys. D: Appl. Phys.* 4 (1971) 613.
22. A. Sussman, *J. Appl. Phys.* 38 (1967) 2738.
23. A. K. Hassan, R. D. Gould, *J. Phys. Condens. Matter* 1 (1989) 6679.
24. M. S. Roy, P. Balraju, Y. S. Deo, R. K. Mishra, V. S. Choudhary, G. D. Sharma, *Solar Energy Materials and Solar Cells* 92 (2008) 1516.
25. S. D. Baranovski, T. Faber, F. Hensel, P. Thomas, J. *Phys. Condens. Matter* 9 (1997) 2699.
26. N. V. Malm, R. Schmechel, H. V. Seggern, *J. Appl. Phys.* 89 (2001) 5559.
27. P. D. Townsend, R. H. Friend, *Phys. Rev. B* 40 (1989) 3112.
28. F. Gutman, L. E. Lyons, *Organic Semiconductors* (1967), (New York, Wiley) .
29. R. D. Gould, *J. Appl. Phys.* 53, 3353 (1982).
30. Cherif Dridi, Maha Benzarti-Ghedira, Francis Vocanson, Rafik Ben Chaabane, Joel Davenas and Hafedh and Ben Ouada, *Semicond. Sci. Technol.* 24, 105007 (2009).
31. Rashmi, A. K. Kapoor, S. Annapoorni, V. Kumar, *Semicond. Sci. Technol.* 23, 035008 (2008).
32. K. Prem Nazeer, Sheeba Anu Jacob, M. Thamilselvan, D. Mangalaraj, Sa K Narayandass and Junsin Yi, *Polymer International* 53 (2004) 898.
33. V. Kumar, S. C. Jain, A. K. Kapoor, J. Poortmans, R. Mertens, *J. Appl. Phys.* 94 (2003) 1283.
34. T. Mori, E. Sugimura, T. Mizutani, *J. Phys. D: Appl. Phys.* 26 (1993) 452.
35. N. Karl, K. H. Kraft, J. Marktanner, *Synth. Met.* 109 (2000) 181.
36. P. W. M. Blom, M. C. J. M. Vissenberg, *Appl. Phys. Lett.* 68 (1996) 3308.
37. L. Bozano, A. Cartera, J. C. Scott, G. G. Malliaras, P. J. Brock, *Appl. Phys. Lett.* 74 (1999) 1132.
38. P. W. M. Blom, C. Tanase, D. M. de Leeuw, R. Coehoorn, *Appl. Phys. Lett.* 86 (2005) 092105.
39. D. Braun, *J. Polym. Sci. B* 41 (2003) 2622.
40. T. Basova, A. G. Gürek, V. Ahsen, A. K. Ray, *Organic Electronics* 8 (2007) 784.
41. Raji Koshy, C. S. Menon, *J. Nano- Electron. Phys.* 3 (2011) 36.
42. S. Mammen, C. S. Menon, N. V. Unnikrishnan, *Materials Science-Poland* 23 (2005) 707.
43. P. R. Binu, C. M. Joseph, K. S. kumar, C. S. Menon, *Materials Letters* 57 (2002) 739.
44. G. B. Kamath, C. M. Joseph, C. S. Menon, *Materials Letters* 57 (2002) 730